King Saud University

Saudi Dental Journal

www.ksu.edu.sa
www.sciencedirect.com

ORIGINAL ARTICLE

Effects of aging and light-curing unit type on the volume and internal porosity of bulk-fill resin composite restoration

Afnan O. Al-Zain [a],*, **Elaf A. Alboloshi** [b,1], **Walaa A. Amir** [b,1], **Maryam A. Alghilan** [c], **Eliseu A. Münchow** [d]

[a] *Restorative Dentistry Department, Faculty of Dentistry, King Abdulaziz University, P. O. Box 80209, Jeddah 21589, Saudi Arabia*
[b] *Faculty of Dentistry, King Abdulaziz University, P. O. Box 80209, Jeddah 21589, Saudi Arabia*
[c] *Restorative and Prosthetic Dental Sciences Department, College of Dentistry, King Saud bin Abdulaziz University for Health Sciences, Riyadh, Saudi Arabia, Ministry of National Guard-Health Affairs, Riyadh, Saudi Arabia*
[d] *Department of Conservative Dentistry, School of Dentistry, Federal University of Rio Grande do Sul, Porto Alegre RS, Brazil*

Abstract This study explores the effects of aging (thermal cycling and cyclic loading–TC/CL) and different light-curing unit (LCU) types on the volume characteristics and internal porosity of a bulk-fill resin-based composite restoration. Occlusal cavities ($4 \times 4 \times 3$ mm) were prepared on extracted human molars (n = 5). Tetric N-Bond Universal was applied, and the cavities were restored using Tetric-N-Ceram Bulk Fill. Photoactivation was performed using a quartz-tungsten halogen (QTH) or a multiple-emission peak light-emitting diode (MLED). Digital images for all restorations were obtained using microcomputed tomography (micro-CT) before (baseline) and after (post-aging) TC/CL (5,000 TC cycles in 5–55 °C baths and a dwell time of 30 s followed by 10,000 sinusoidal CL load cycles in an Instron B3000 at 2 Hz and 10–110 N) and storage (37 °C) for three months. For the micro-CT analysis, three-dimensional images were used to determine the restoration volume and internal porosity. Data were analyzed using a two-way ANOVA and Tukey's test (p < 0.05). Restorations photoactivated with QTH exhibited a higher object volume than the LED group at baseline and in post-aging conditions without any significant differences in the other evaluated characteristics. All volume/porosity characteristics increased considerably after TC/CL aging, except for the object volume of the QTH group and the closed

* Corresponding author.
E-mail addresses: alzain@kau.edu.sa (A.O. Al-Zain), ealboloshi@stu.kau.edu.sa (E.A. Alboloshi), wamir@kau.edu.sa (W.A. Amir), ghilanm@ksau-hs.edu.sa (M.A. Alghilan), eliseu.munchow@ufrgs.br (E.A. Münchow).
[1] Second and third authors contributed equally to the paper.

porosity of the MLED group. The change in all the volume/porosity characteristics between both LCU groups after TC/CL were not significantly different. Thus, the aging process simulated herein increased the volume and porosity characteristics of the bulk-fill restoration, and no significant differences were obtained between the QTH and MLED equipment.

1. Introduction

Resin-based composites (RBCs) are widely used to restore teeth that have a loss of dental structure (Alvanforoush et al., 2017). Despite their adequate strength and wear resistance, RBCs undergo hydrolytic degradation during oral function (Drummond et al., 2009), which impairs the clinical longevity of restorations (Ilie et al., 2017). Additionally, fatigue can be initiated from internal flaws created during the fabrication of large restorations (Astvaldsdottir et al., 2015). Thus, to acquire optimal strength, RBCs require appropriate photoactivation, which depends on features such as radiant exposure and the type of light-curing unit (LCU) used (Leprince et al., 2013; Rueggeberg et al., 2017).

The LCUs currently used in daily routines consist of light-emitting diodes (LEDs), which replaced the traditionally used quartz-tungsten-halogen (QTH) equipment (Rueggeberg et al., 2017). QTH-based LCUs utilize spectral emission ranging from 375 to 510 nm, and they exhibit a relatively uniform emission beam profile (Al-Zain et al., 2019b; Rueggeberg et al., 2017). Conversely, multiple-emission peak LEDs (MLED) have a spectral emission comprising two peaks (in the violet range [380–425 nm] and the blue range [420–520 nm]) (Al-Zain et al., 2019b; Rueggeberg et al., 2017) with chips positioned side-by-side, which results in a nonuniform irradiance beam profile (Al-Zain et al., 2019a; Price et al., 2011; Rueggeberg et al., 2017). Considering the incomplete conversion of monomers in RBC restorations (70%–75% level) (Ferracane and Condon, 1990; Leprince et al., 2013), the release of unreacted monomers may create postcure pores and voids within the body of restorations (Balthazard et al., 2014; Bonilla et al., 2012; Ilie et al., 2017; Olmez et al., 2004). Accordingly, internal porosity may become areas of stress concentration, thereby leading to the propagation of cracks and, ultimately, to restoration failure (Jorgensen, 1980).

Among the currently available RBCs, bulk-fill materials possess the advantage of an extended depth of polymerization, i.e., they can be applied at thicknesses of 4–5 mm, which differs from conventional RBCs (Chesterman et al., 2017). While the bulk application of a larger volume of material may reduce the occurrence of internal flaws/defects (Rosa de Lacerda et al., 2019), a thicker increment may induce uneven polymerization. This study makes a novel contribution to the literature by exploring the impact of light curing type and the combined TC and CL aging conditions on a bulk-filled restoration volume and internal porosity. To our knowledge no study investigated this before and more scientific evidence is needed in the literature. Hence, this study investigates the effects of the LCU type and aging on the volume characteristics and internal porosity of a bulk-fill restoration. The null hypothesis is that aging and the LCU type do not affect the volume or the porosity characteristics.

2. Materials and methods

2.1. Teeth preparation and restoration

Sound human molars were obtained after approval by the local Research Ethics Committee of the Faculty of Dentistry at King Abdulaziz University (No. 135–11–18). The teeth were disinfected, stored in normal saline (0.9% sodium chloride) until use, and then embedded in self-polymerizing acrylic resin. The cusp tips of each tooth were wet-grounded with 400-grit SiC to obtain flat occlusal surfaces; the dentin was left intact at the center of the tooth. Occlusal cavities (4 mm length × 4 mm width × 3 mm height) were centrally prepared using a round-ended carbide bur (0.12 mm) with a multifunctional milling machine (Paraskop®, BEGO, Bremen, Germany). All samples were randomly separated into two groups according to the LCU (n = 5): light cured using (1) an MLED (Bluephase N, Ivoclar Vivadent, Schaan, Liechtenstein) that possesses a 9-mm diameter guide tip, ~840 mW power, and 1325 mW/cm² irradiance and (2) a QTH (Astralis 3, Ivoclar Vivadent, Schaan, Liechtenstein) that possesses a 7-mm diameter guide tip, ~325 mW power, and 840 mW/cm² irradiance.

Each cavity was treated using Tetric N-Bond Universal adhesive (Ivoclar Vivadent, Schaan, Liechtenstein) in self-etch mode; it was rubbed into the cavity for 20 s, air-dried, and light cured for 10 s using the standard mode. Each restoration was prepared by packing 3 mm of Tetric-N-Ceram Bulk Fill (Ivoclar Vivadent, Schaan, Liechtenstein) into the cavities; Mylar strip and glass slide were positioned on the restoration to extrude any excess material. A description of the materials used is given in Table 1. Photoactivation was conducted using the respective LCU in the standard mode for 20 s according to the manufacturer's instructions, and the light guide tip was kept centered over the cavity. A mechanical arm was used to standardize the distance at 2 mm (Al-Zain et al., 2019b). The irradiance output from each LCU was measured in triplicate at a 2 mm distance for 20 s using a spectrometer (Managing Accurate Resin Curing-Light Corrector; BlueLight Analytics, Halifax, Canada). The total radiant exposure received at the top of the restoration was 26 J/cm² (MLED) or 18 J/cm² (QTH).

2.2. Micro-CT analysis

All restored teeth were scanned in three dimensions using microcomputed tomography (micro-CT; SkyScan 1272, Bruker microCT, Kontich, Belgium) at two distinct moments: before aging (baseline) and after the aging simulation (post-aging). For the baseline, samples were restored, immediately scanned, then subjected to TC/CL and stored. Samples were stored in saline, stored in dark conditions in the incubator (37 °C) for three months, and then scanned post-aging. The

Table 1 Descriptions of the universal adhesive and bulk-fill resin composite used in the study.

Material	Manufacturer	Shade	Composition	Lot number
Tetric N-Bond Universal	Ivoclar Vivadent, Shaan, Liechtenstein	U	Resin monomers (HEMA, 10-MDP, Bis-GMA, MCAP and D3MA), ethanol, water, highly disperse SiO_2 fillers, photoinitiator (CQ)	X36453
Tetric N-Ceram Bulk Fill	Ivoclar Vivadent, Shaan, Liechtenstein	IVA	Resin monomers (Bis-GMA and UDMA) and fillers (Ba–Al–Si-glass, prepolymer fillers and spherical mixed oxide)	X48519

HEMA: 2-hydroxyethyl methacrylate; 10-MDP: 10-methacryloyloxydecyl-dihydrogen-phosphate; Bis-GMA: bisphenol-A glydidyl methacrylate; MCAP: methacrylate carboxylic acid polymer; D3MA: decandiol dimethacrylate; SiO_2: silica dioxide; CQ: camphorquinone; UDMA: urethane dimethacrylate.

acquisition parameters for the micro-CT analysis are as follows: aluminum and copper filter, nine camera pixel size, 100 source voltage and current, and flat-field correction. The scans were reconstructed using NRecon (Bruker microCT, Kontich, Belgium) to generate three-dimensional (3D) images. The baseline and post-aging 3D image sets were analyzed using Data-Viewer and CT Analyzer (Bruker microCT, Kontich, Belgium) by an independent expert. The 3D volumetric quantitative analysis was initiated by rotating and aligning the images in DataViewer. The 3D-oriented images were then processed using the CT Analyzer by applying thresholding, despeckling, and bitwise operation functions to delineate and segment the restoration. The segmented restoration volume and porosity values were then obtained using the built-in functions for 3D analysis. The segmented restorations were rendered using CTvox (Bruker microCT, Kontich, Belgium), where the volume and pores were evaluated. In total, four response variables were investigated in this study: object volume, number of closed pores, volume of closed pores, and closed porosity. The measured values were exported to Excel (Microsoft, Redmond, Washington, USA) spreadsheets to further analyze the volumetric and porosity changes in the restoration between the baseline and post-aging conditions.

2.3. Aging simulation (TC/CL)

After the micro-CT baseline measurements, all samples underwent thermal cycling using a thermocycler (THE-1100/1200, SD Mechatronic, Feldkirchen-Westerham, Germany). The specimens were subject to 5,000 cycles in alternating baths of 5 °C and 55 °C with a dwell time of 30 s and a transfer time of 10 s. The samples were then subjected to cyclic loading under dry conditions using a dynamic mechanical testing machine with a flat load cell (Instron B3000, Noorwood, Massachusetts, USA); a 2 Hz frequency and a range of 10–110 N were used for 10,000 cycles (Al-Shehri et al., 2017; Nishigori et al., 2014; Turssi et al., 2006). After the TC/CL process, all samples were stored in saline under dark conditions in the incubator for three months (37 °C).

2.4. Statistical analysis

Data on the volume and porosity of the restorations were statistically analyzed using a two-way analysis of variance followed by Tukey's *post hoc* test. Data on the change in the restoration volume and internal porosity obtained with each

LCU were analyzed using the Mann–Whitney rank-sum test. The significance level of all analyses was set at $\alpha = 0.05$. Statistical analyses were performed using SigmaPlot, version 12.0 (SPSS Inc., Chicago, Illinois, USA).

3. Results

Table 2 shows the mean values of the tested volume and porosity characteristics. Restorations that were photoactivated with QTH exhibited a higher object volume than those using MLED under both baseline and post-aging conditions ($p \leq 0.004$) without any significant difference in the other characteristics ($p \geq 0.085$). All volume-porosity characteristics increased after aging ($p \leq 0.017$) except for the object volume when using QTH ($p = 0.089$) and the closed porosity when using MLED ($p = 0.073$), which exhibited similar values for the baseline and post-aging conditions.

The volume and porosity characteristics increased considerably after aging for all MLED-activated restorations and the majority (75%) of the QTH-activated restorations without significant differences between the groups ($p \geq 0.301$). Representative micro-CT 2D and 3D rendered segmented images of restorations cured using the MLED- and QTH-based LCUs are presented in Fig. 1. Overall, restorations from the MLED group exhibited a lower porosity than the QTH group.

4. Discussion

This study used two LCUs with distinct emission profiles to verify whether a QTH or MLED unit can alter the bulk characteristics of a bulk-fill RBC. Overall, only one characteristic (object volume) differed between the groups, and aging affected all the investigated characteristics, thereby partially rejecting the study's null hypothesis.

Aspects such as the LCU position, RBC type, and shade were standardized to minimize any confounding factors. The teeth were flattened to allow all restoration areas to receive a similar amount of irradiance (Alqudaihi et al., 2019); one-shot curing was ensured for all the restorations (Al-Zain et al., 2018; Al-Zain and Platt, 2020; Eshmawi et al., 2018); the light guide tip was positioned centrally to standardize the delivery of energy (Al-Zain et al., 2018; Price et al., 2011; Shimokawa et al., 2018); and a curing distance of 2 mm was used to simulate a clinical setting (Al-Zain et al., 2018; Price et al., 2011). Thus, we controlled many of the potential important operational aspects that may affect the polymerization of

Table 2 Mean and standard deviation (SD) values for the characteristics tested in the study and the respective percentage change median (minimum/maximum) values after thermal-cycling and cyclic loading (TC/CL) aging.

Aging condition	Object volume (mm³)*		Number of closed pores*		Volume of closed pores (mm³)*		Closed porosity (%)*	
	LED	QTH	LED	QTH	LED	QTH	LED	QTH
Baseline	17.1 (3.2) [B, b]	35.4 (7.0) [A, a]	1377 (1050) [B, a]	1672 (1733) [B, a]	0.07 (0.07) [B, a]	0.10 (0.08) [B, a]	0.4 (0.3) [A, a]	0.3 (0.3) [B, a]
Post-aging	30.5 (5.4) [A, b]	43.6 (7.3) [A, a]	5390 (2553) [A, a]	7948 (2819) [A, a]	0.28 (0.16) [A, a]	0.47 (0.34) [A, a]	0.9 (0.4) [A, a]	1.0 (0.7) [A, a]
Change (%) after TC/CL[§]	93 (25/119)	−0.1 (-4/84)	260 (173/796)	684 (116/16039)	287 (128/1116)	473 (72/6566)	125 (32/524)	244 (-6/6502)
	p = 0.408		p = 0.301		p = 0.421		p = 0.424	

LED: light-emitting diode curing unit; QTH: quartz-tungsten halogen curing unit; Baseline: before TC/CL aging; Post-aging: after TC/CL aging.
* Distinct uppercase (comparisons in the columns) and lowercase (comparisons in the rows) letters indicate statistically significant differences between the tested groups ($p < 0.05$); Two Way Analysis of Variance and Tukey *post hoc* test.
§ There were not statistical significant differences between LED and QTH groups regardless of the tested characteristics ($p > 0.05$); Mann-Whitney Rank Sum Test.
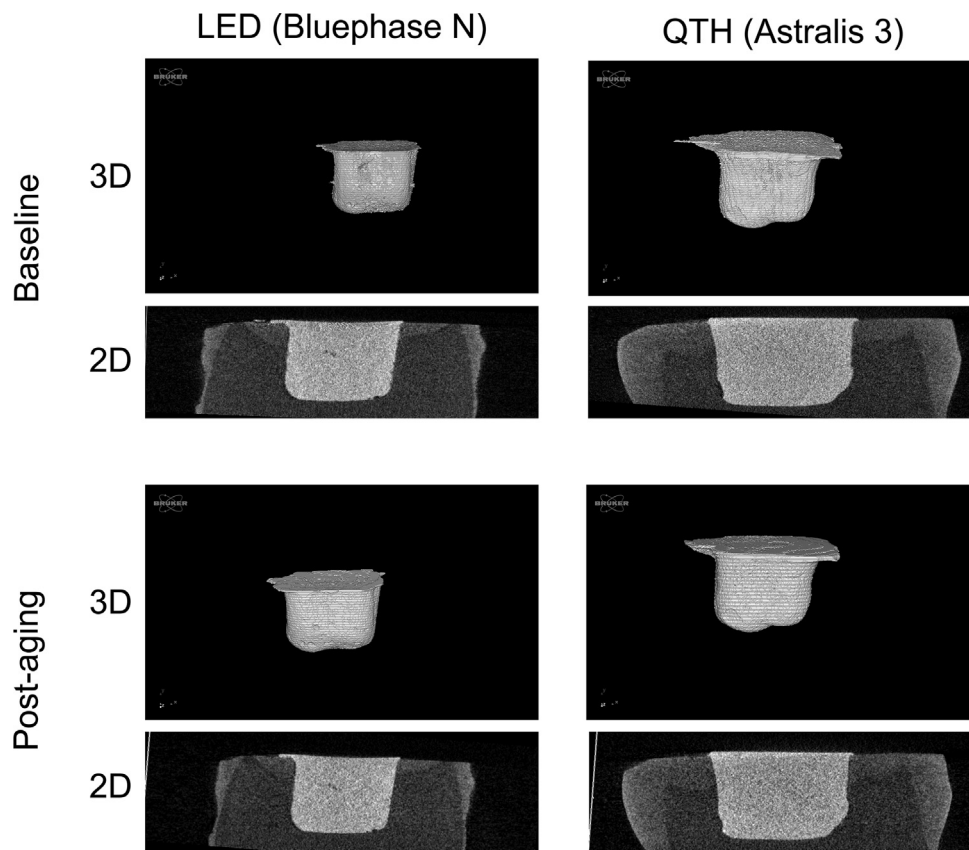

Fig. 1 Representative micro-CT 2D and 3D rendered segmented images of a bulk-fill restoration before (baseline) and after (post-aging) thermal cycling and a cyclic loading aging simulation for both of the tested light-curing units: a light-emitting diode (LED) and a quartz-tungsten-halogen (QTH).

the restorations, thereby enabling the acquisition of accurate data.

The MLED equipment tested in this study has a nonhomogenous irradiance beam profile, which enables different blue and violet photons and a radiant distribution across the LCU tip (Shimokawa et al., 2018). According to some studies (Al-Zain et al., 2019a; Al-Zain et al., 2018; Al-Zain and Platt, 2020; Eshmawi et al., 2018), up to 95% of the radiant exposure/irradiance may be lost from the top to the bottom areas during light transmission through RBCs as thin as 1–2 mm.

Similarly, ~10% of the light emitted by an LCU reaches the bottom areas of a 4-mm bulk-fill RBC (Shimokawa et al., 2018), and a violet spectral emission may no longer be detected at the bottom of 2-mm-deep specimens (Al-Zain et al., 2018; Al-Zain et al., 2019b). Therefore, we may expect a similar loss of radiant exposure/irradiance in the 3-mm bulk-fill specimens in our study. However, considering that the polymerization level depends on the activated photoinitiator, LCUs with a relatively homogenous light emission (e.g., QTH) are preferable to LCUs with a nonhomogeneous irradiance distribution (e.g., LED).

According to Giorgi et al. (2015), the polymerization level of RBCs was not influenced, even after successive photoactivations using multiple or single irradiation protocols (Giorgi et al., 2015). The QTH equipment resulted in a similar polymerization efficacy at the top and bottom increments of the RBC. However, new-generation LEDs were considered better alternatives for the polymerization of bulk-fill RBCs than QTH (Pirmoradian et al., 2020), particularly for polymerizing materials with novel initiation systems (e.g., Ivocerin), as tested herein. Previous studies exhibited significant differences between the mean degree of conversion (DC) at the top and bottom surfaces of an RBC containing diphenyl (2,4,6-trimethylbenzoyl) phosphine oxide (TPO) as the photoinitiator when cured using QTH or MLED; however, the mean DC was above 67% (Al-Zain et al., 2018). Other studies also showed that the mean DC of the same RBC containing TPO was above 63% upon the use of QTH and several LEDs (Al-Zain et al., 2019b). Surprisingly, there were no relevant differences in this study concerning the LCU type, particularly when considering the change in the restoration volume and internal porosity.

It has been established that 16 J/cm^2 is the minimum energy necessary to achieve appropriate polymerization (Leprince et al., 2013; Price et al., 2011), and restorations in our study received radiant exposure above this level. This may have contributed to the effective activation of free radicals and adequate polymerization for all restorations. Another aspect is related to the type of photoinitiator for the tested RBC (Ivocerin), which has a higher absorption capacity in the violet range than in the blue range, and it can be activated using a single LED or MLED (Rueggeberg et al., 2017). The violet and blue LED chips are positioned side-by-side; thus, they emit nonhomogeneous light. However, a sufficient amount of photoinitiators may have been excited, thereby generating sufficient free radicals and satisfactory polymerization (Al-Zain et al., 2019a; Price et al., 2015; Rueggeberg et al., 2017). More importantly, Tetric N-Ceram Bulk Fill comprises photoinitiators other than Ivocerin, such as TPO and the traditionally used camphorquinone, and this intrinsic composition may guarantee an adequate conversion of monomers, regardless of the LCU type (Pirmoradian et al., 2020).

In our study, the restored teeth were thermally cycled for 5,000 cycles, which simulated 6 months of oral function, followed by 10,000 sinusoidal cyclic loadings (Al-Shehri et al., 2017). Considering the DC, a previous study showed that monomer conversion improved after 4,000 cycles of TC (Ghavami-Lahiji et al., 2018). Thus, we may assume that the restoration temperature increased during aging (Truffier-Boutry et al., 2006) and RBC heating at 55 °C (i.e., the temperature level close to the glass transition [Tg]) may have driven the continuation of the polymerization process

(Truffier-Boutry et al., 2006), thereby causing radical recombination and enhanced polymerization. However, these inferences may vary with different photoactivation protocols, which warrants further investigation of this topic.

Other aspects should be considered regarding the effects of distinct LCUs in the photoactivation of RBCs, such as the development of polymerization stress. Notably, QTH units tend to deliver lower energy. Considering the lower radiant exposure of this group in our study, we may assume that polymerization stress is less intense at the body of restorations photoactivated using QTH (Munchow et al., 2018). This may explain the increased object volume for this group compared with the MLED group. The negative effects of polymerization stress may also depend on the chemical composition of the material; however, bulk-fill RBCs represent one of the most effective formulations for the significant reduction in and control of stress development (Meereis et al., 2018). Therefore, despite the LCU type, it is feasible to assume that all restorations prepared in our study contributed to the same level of polymerization stress, which justifies the similar volume/porosity characteristics demonstrated herein.

The clinical relevance of our findings relates to the fact that nonuniform beam profiles from different LCUs may not affect restoration volume and internal porosity after aging, thereby enabling clinicians to use a QTH or MLED without compromising restoration quality. A limitation of this study is that only two types of LCUs were investigated; therefore, future studies that test other equipment, delivering similar radiant exposure values to specimens, and different types of RBCs are necessary.

5. Conclusions

Aging increased all volume and porosity characteristics of a bulk-fill restoration without any significant differences between the LCUs. However, when considering the object volume property only, the MLED unit is preferable over QTH for polymerizing bulk-fill restoratives.

Funding

Ethical approval

The manuscript titled "Effects of aging and light-curing unit type on the volume and internal porosity of a bulk-fill resin composite restoration" with proposal no. 135-11-18 was approved by the Research ethical committee at King Abdulaziz University Faculty of Dentistry.

Declaration of Competing Interest

The authors declare that they have no known competing financial interests or personal relationships that could have appeared to influence the work reported in this paper.

References

Al-Shehri, E.Z., Al-Zain, A.O., Sabrah, A.H., Al-Angari, S.S., Al Dehailan, L., Eckert, G.J., Ozcan, M., Platt, J.A., Bottino, M.C., 2017. Effects of air-abrasion pressure on the resin bond strength to zirconia: A combined cyclic loading and thermocycling aging study. Restor. Dent. Endod. 42, 206–215.

Al-Zain, A.O., Eckert, G.J., Lukic, H., Megremis, S.J., Platt, J.A., 2018. Degree of conversion and cross-link density within a resin-matrix composite. J. Biomed. Mater. Res. B Appl. Biomater. 106, 1496–1504.

Al-Zain, A.O., Eckert, G.J., Lukic, H., Megremis, S., Platt, J.A., 2019a. Polymerization pattern characterization within a resin-based composite cured using different curing units at two distances. Clin. Oral. Investig. 23, 3995–4010.

Al-Zain, A.O., Eckert, G.J., Platt, J.A., 2019b. The influence of distance on radiant exposure and degree of conversion using different light-emitting-diode curing units. Oper. Dent. 44, E133–E144.

Al-Zain, A.O., Platt, J.A., 2020. Effect of light-curing distance and curing time on composite microflexural strength. Dent. Mater. J. 40, 202–208.

Alqudaihi, F.S., Cook, N.B., Diefenderfer, K.E., Bottino, M.C., Platt, J.A., 2019. Comparison of internal adaptation of bulk-fill and increment-fill resin composite materials. Oper. Dent. 44, E32–E44.

Alvanforoush, N., Palamara, J., Wong, R.H., Burrow, M.F., 2017. Comparison between published clinical success of direct resin composite restorations in vital posterior teeth in 1995–2005 and 2006–2016 periods. Aust. Dent. J. 62, 132–145.

Astvaldsdottir, A., Dagerhamn, J., van Dijken, J.W., Naimi-Akbar, A., Sandborgh-Englund, G., Tranaeus, S., Nilsson, M., 2015. Longevity of posterior resin composite restorations in adults – A systematic review. J. Dent. 43, 934–954.

Balthazard, R., Jager, S., Dahoun, A., Gerdolle, D., Engels-Deutsch, M., Mortier, E., 2014. High-resolution tomography study of the porosity of three restorative resin composites. Clin. Oral. Investig. 18, 1613–1618.

Bonilla, E.D., Stevenson, R.G., Caputo, A.A., White, S.N., 2012. Microleakage resistance of minimally invasive class I flowable composite restorations. Oper. Dent. 37, 290–298.

Chesterman, J., Jowett, A., Gallacher, A., Nixon, P., 2017. Bulk-fill resin-based composite restorative materials: A review. Br. Dent. J. 222, 337–344.

Drummond, J.L., Lin, L., Al-Turki, L.A., Hurley, R.K., 2009. Fatigue behaviour of dental composite materials. J. Dent. 37, 321–330.

Eshmawi, Y.T., Al-Zain, A.O., Eckert, G.J., Platt, J.A., 2018. Variation in composite degree of conversion and microflexural strength for different curing lights and surface locations. J. Am. Dent. Assoc. 149, 893–902.

Ferracane, J.L., Condon, J.R., 1990. Rate of elution of leachable components from composite. Dental Mater.: Off. Publication Acad. Dental Mater. 6, 282–287.

Ghavami-Lahiji, M., Firouzmanesh, M., Bagheri, H., Kashi, T.S.J., Razazpour, F., Behroozibakhsh, M., 2018. The effect of thermocycling on the degree of conversion and mechanical properties of a microhybrid dental resin composite. Restor. Dent. Endod. 43, e26.

Giorgi, M.C., Theobaldo, J., Lima, D.A., Marchi, G.M., Ambrosano, G.M., Aguiar, F.H., 2015. Influence of successive light-activation on degree of conversion and knoop hardness of the first layered composite increment. Acta. Odontol. Scand. 73, 126–131.

Ilie, N., Hilton, T.J., Heintze, S.D., Hickel, R., Watts, D.C., Silikas, N., Stansbury, J.W., Cadenaro, M., Ferracane, J.L., 2017. Academy of dental materials guidance-resin composites: Part I-mechanical properties. Dental Mater.: Off. Publication Acad. Dental Mater. 33, 880–894.

Jorgensen, K.D., 1980. Restorative resins: Abrasion vs. mechanical properties. Scand. J. Dent. Res. 88, 557–568.

Leprince, J.G., Palin, W.M., Hadis, M.A., Devaux, J., Leloup, G., 2013. Progress in dimethacrylate-based dental composite technology and curing efficiency. Dental Mater.: Off. Publication Acad. Dental Mater. 29, 139–156.

Meereis, C.T.W., Munchow, E.A., da Rosa, W.L.D.O., da Silva, A.F., Piva, E., 2018. Polymerization shrinkage stress of resin-based dental materials: A systematic review and meta-analyses of composition strategies. J. Mech. Behav. Biomed. Mater. 82, 268–281.

Munchow, E.A., Meereis, C.T.W., da Rosa, W.L.D.O., da Silva, A.F., Piva, E., 2018. Polymerization shrinkage stress of resin-based dental materials: A systematic review and meta-analyses of technique protocol and photo-activation strategies. J. Mech. Behav. Biomed. Mater. 82, 77–86.

Nishigori, A., Yoshida, T., Bottino, M.C., Platt, J.A., 2014. Influence of zirconia surface treatment on veneering porcelain shear bond strength after cyclic loading. J. Prosthet. Dent. 112, 1392–1398.

Olmez, A., Oztas, N., Bodur, H., 2004. The effect of flowable resin composite on microleakage and internal voids in class II composite restorations. Oper. Dent. 29, 713–719.

Pirmoradian, M., Hooshmand, T., Jafari-Semnani, S., Fadavi, F., 2020. Degree of conversion and microhardness of bulk-fill dental composites polymerized by LED and QTH light curing units. J. Oral. Biosci. 62, 107–113.

Price, R.B., Ferracane, J.L., Shortall, A.C., 2015. Light-curing units: A review of what we need to know. J. Dent. Res. 94, 1179–1186.

Price, R.B., Labrie, D., Whalen, J.M., Felix, C.M., 2011. Effect of distance on irradiance and beam homogeneity from 4 light-emitting diode curing units. J. (Can. Dental Assoc.) 77, b9.

Rosa de Lacerda, L., Bossardi, M., Mitterhofer, W.J.S., de Carvalho, F.G., Carlo, H.L., Piva, E., Munchow, E.A., 2019. New generation bulk-fill resin composites: Effects on mechanical strength and fracture reliability. J. Mech. Behav. Biomed. Mater. 96, 214–218.

Rueggeberg, F.A., Giannini, M., Arrais, C.A.G., Price, R.B.T., 2017. Light curing in dentistry and clinical implications: A literature review. Braz. Oral. Res. 31, e61.

Shimokawa, C.A.K., Turbino, M.L., Giannini, M., Braga, R.R., Price, R.B., 2018. Effect of light curing units on the polymerization of bulk fill resin-based composites. Dental Mater.: Off. Publication Acad. Dental Mater. 34, 1211–1221.

Truffier-Boutry, D., Demoustier-Champagne, S., Devaux, J., Biebuyck, J.J., Mestdagh, M., Larbanois, P., Leloup, G., 2006. A physico-chemical explanation of the post-polymerization shrinkage in dental resins. Dental Mater.: Off. Publication Acad. Dental Mater. 22, 405–412.

Turssi, C.P., Ferracane, J.L., Ferracane, L.L., 2006. Wear and fatigue behavior of nano-structured dental resin composites. J. Biomed. Mater. Res. B Appl. Biomater. 78, 196–203.